Optical and Acoustical Methods in Science and Technology

Tm^{3+}/Ho^{3+}-Doped ASE Fibre Source for Mid-Infrared Sensor Applications

D. Dorosz*, J. Żmojda, M. Kochanowicz, P. Miluski and J. Dorosz
Department of Optoelectronics and Lighting Technology, Białystok University of Technology
Wiejska 45, 15-351 Białystok, Poland

The infrared emission of Tm^{3+}/Ho^{3+}-doped antimony–silicate optical fiber has been presented. Luminescence at 2.1 μm corresponding to ${}^5I_7 \rightarrow {}^5I_8$ transition in holmium was obtained by energy transfer between Tm^{3+} and Ho^{3+} ions. According to the Förster–Dexter theory, the efficiency of energy transfer of the ${}^3F_4$ (Tm^{3+}) $\rightarrow {}^5I_7$ (Ho^{3+}) transition was calculated. The optimization of the activator content and the donor (Tm^{3+})/acceptor (Ho^{3+}) ions concentration ratio were conducted with the purpose of maximizing the efficiency of energy transfer. It made possible to select best-suited glass which was used to manufacture double-clad optical fiber. Strong and narrow bands of amplified spontaneous emission which formed as a result of energy transfer between thulium and holmium ions were observed in the fiber under exciting with radiation at 795 nm wavelength.

PACS: 42.81.–i, 42.79.Ag, 33.20.Kf

1. Introduction

Efficient fibers sources of 2 μm radiation are required for a range of applications in medicine [1], remote sensing [2, 3] and materials processing [4, 5]. Moreover, radiation above 1.5 μm is widely considered as eye-safe, hence the possibility of constructing laser rangefinders and radars [6, 7]. There are two lanthanide ions that have been responsible for the emission in the 2 μm region, namely from the Tm^{3+}: ${}^3F_4 \rightarrow {}^3H_6$ transition and the Ho^{3+}: ${}^5I_7 \rightarrow {}^5I_8$ transition [8, 9]. Both transitions have the ground state as the lower laser level, and the luminescence spectrum emitted from these transitions is relatively broad. A direct excitation of Tm^{3+} ions from their ground state to the ${}^3H_6$ level takes place as a result of pump radiation absorption at 795 nm and will show emission at 1.8 μm. However, Ho^{3+} cannot directly absorb a pumped beam of commercially available high power laser diodes (795 nm or 976 nm), due to the lack of strong absorption band. Therefore, it is necessary to apply sensitizators like Yb^{3+} and Tm^{3+} ions, which intercede in energy transfer of excitation radiation and making it possible to produce emission at the wavelength of 2 μm.

To achieve a strong luminescence in the range of 1.7–2.2 μm, an optimization of energy transfer efficiency between ions should be carried out by selecting appropriate doping concentration of both the elements and placing them simultaneously in a single glass matrix. Among the materials most frequently used for the purpose of fiber lasers design, the most popular is silicon dioxide (SiO_2) which is characterized by high mechanical and chemical resistance. Unfortunately, due to low solubility of activator ions, as well as high probability of non-radiative decays, the efficiency of energy transfer in such media is low, thus encouraging search for new glasses with relatively low phonon energy which would ensure increased energy transfer between activators. One possible method of producing glasses with desired physicochemical and optical properties involves combining elements with diametrically different phonon oscillation frequencies. As a consequence, combination of relatively low phonon energy with a capability for greater separation of optically active centres in the discussed glasses should allow an effective expansion of spontaneous emission band [10].

In the course of the presented research, the authors performed a synthesis of antimony–silicate glasses doped with Tm^{3+} and Ho^{3+} ions to obtain radiation emission within the range of 1.7–2.2 μm. The actual composition of the core glass in which effective energy transfer $Tm^{3+} \rightarrow Ho^{3+}$ was observed had been determined by optimizing the content of rare earth ions and the Tm^{3+}/Ho^{3+} ion ratio. The glass was used for manufacturing double-clad optical fiber whose luminescent parameters were then evaluated [11].

2. Experiment

Glasses from the system SiO_2–Sb_2O_3–Al_2O_3 doped with 1 mol.% Tm_2O_3 and x mol.% Ho_2O_3 (where $x = 0$, 0.1, 0.2, 0.5, 0.75, 1.0, 1.25 and 1.5) were prepared using high purity reagents (99.99%). Inhomogeneous material (20 g) was molten in an electric furnace at about 1550 °C during 30 min in a platinum crucible. The molten glass was then poured into a preheated stainless steel mould, and subsequently annealed for 12 h at a temperature close to the vitreous transition temperature. Thus obtained samples were cut into specimens of 10 mm × 10 mm × 2 mm, and optically polished for measurements of the absorption and emission spectra. Double-clad active fiber was accomplished by means of the standard rod-

* corresponding author; e-mail: d.dorosz@pb.edu.pl

-in-tube method. The designed antimony–silicate glasses doped with thulium and holmium ions were used as the active core, ensuring the maximum level of luminescence.

Absorption spectra of rare-earth ions doped samples were determined using an Acton Spectra Pro 2300i monochromator in the spectral range of 500–2200 nm. As for the luminescence spectra in the range of 1350–2300 nm, they were measured with a Stelarnet RW--InGaAs-1024X spectrometer, using high power laser diode ($\lambda_p = 795$ nm) as a pump source.

3. Results

3.1. Absorption coefficient

Figure 1a presents the absorption coefficient spectrum of glasses doped with 1 mol.% Tm^{3+}. In the spectral range between 600 and 2200 nm four absorption bands were observed corresponding with transitions from the ground state $^3H_6$ to the excited states $^3F_4$, $^3H_5$, $^3H_4$, $^3F_{2,3}$.

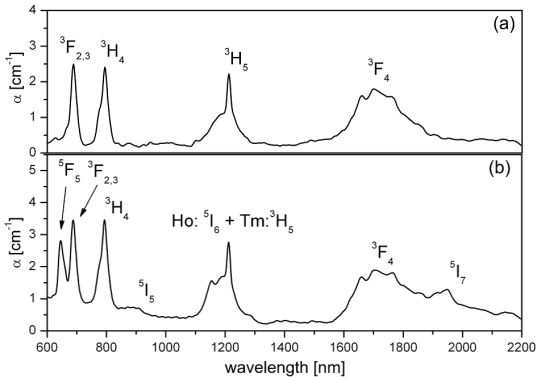

Fig. 1. Absorption coefficient spectra of antimony–silicate glasses doped with (a) 1 mol.% Tm_2O_3, (b) 1 mol.% Tm_2O_3 : 0.75 mol.% Ho_2O_3.

With the introduction of the second element (i.e. holmium) into the matrix, additional absorption bands appeared respectively to the energetic states of its ion quantum structure. Figure 1b shows the absorption coefficient spectrum of the co-doped glass in the proportion 1 mol.% Tm_2O_3 : 0.75 mol.% Ho_2O_3. Observing absorption coefficient spectra in this glass, five bands corresponding with the transitions $^5I_8 \rightarrow {}^5I_7$, $^5I_6$, $^5I_5$, $^5F_5$ related to the presence of Ho^{3+} ions were noted. The level of absorption for individual holmium ion bands increases proportionally to the growth of concentration of the activator, whereas the spectral location of transition maximum remains unchanged.

3.2. Luminescence spectra

Figure 2 presents the obtained luminescence spectra of glasses activated by 1% Tm_2O_3 as well as of those doped with 1% Tm_2O_3 : 0.75% Ho_2O_3. The sample doped exclusively with thulium ions was characterized by a strong luminescence line with the maximum emission reached at the wavelength of 1810 nm and significantly lower emission in the band of 1.46 μm. The introduction of holmium ions lowered the luminescence level corresponding with the $^3F_4 \rightarrow {}^3H_6$ (Tm^{3+}) quantum transition, at the same time causing luminescence line to appear at the 2 μm region in correspondence with the transition $^5I_7 \rightarrow {}^5I_8$ in the energy-level structure of the holmium ion.

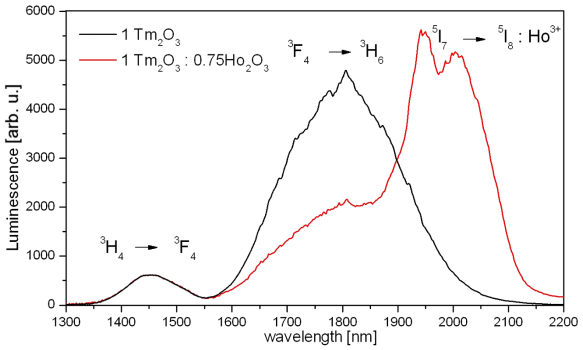

Fig. 2. Comparison of the luminescence spectra of singly Tm^{3+} doped and Tm^{3+}/Ho^{3+} codoped antimony–silicate glass samples under 795 nm LD excitation.

Producing luminescence at the wavelength within the band of 2 μm was possible owing to the quasi-resonant non-radiative energy transfer $Tm^{3+} \rightarrow Ho^{3+}$. As a result of effective $^3F_4$ (Tm^{3+}) and $^5I_7$ (Ho^{3+}) multiplet coupling, the highest level of luminescence was achieved in the glass co-doped with 1% Tm_2O_3 : 0.75% Ho_2O_3.

3.3. Mechanism of energy transfer

Relying on the spectrum of absorption coefficient, a simplified model of energetic states which ensued in the produced antimony glasses doped with both thulium and holmium ions was created (Fig. 3). The diagram presents fundamental mechanisms of energy transfer occurring as a result of interaction between the active medium and radiation at the wavelength within the band of 795 nm, corresponding with the $^3H_6 \rightarrow {}^3H_4$ transition.

Laser level $^3F_4$ (Tm^{3+}) is populated as an effect of depopulation of the $^3H_4$ multiplet in the course of multi--phonon relaxation $^3H_4 \rightarrow {}^3H_5 \rightarrow {}^3F_4$ (dotted line) and cross-relaxation (CR). Ions gathered on this level in effect of transmission to the ground state $^3H_6$ (Tm^{3+}) can emit an energy quantum in the form of photon emission within the band of 1810 nm, as well as transfer a portion of their energy to the holmium ions in the process of quasi-resonant energy transfer (ET). Following the $^3F_4$ (Tm^{3+}) $\rightarrow {}^5I_7$ (Ho^{3+}) transition, population of the $^5I_7$ level increases and a band of spontaneous emission appears at the wavelength within the band of 2010 nm. These mechanisms can be described by the following dependences:

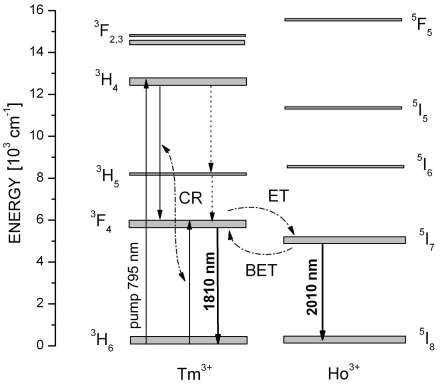

Fig. 3. Mechanisms of the energy transfer between Tm^{3+} and Ho^{3+} in antimony–silicate glasses.

$$\text{CR: } (\mathrm{Tm}^{3+})^3H_4 \rightarrow {}^3F_4, \quad (\mathrm{Tm}^{3+})^3H_6 \rightarrow {}^3F_4, \tag{1}$$

$$\text{ET: } (\mathrm{Tm}^{3+})^3F_4 \rightarrow {}^3H_6, \quad (\mathrm{Ho}^{3+})^5I_8 \rightarrow {}^5I_7. \tag{2}$$

Furthermore, because of the spatial overlap between multiplets $^3F_4$ and $^5I_7$ (energy difference between the levels is *ca.* 400 cm^{-1}) and with a relatively large number of acceptor ions (Ho^{3+}), the phenomenon of back energy transfer (BET) may occur, and the probability of acceptor–acceptor diffusion transfer is elevated, which artificially extends the lifetime of electrons at the laser level $^5I_7$, ultimately leading to lower efficiency of quantum emission within the band of about 2 μm.

3.4. Analysis of cross-sections and energy transfer mechanisms

Analysis of energy transfer between Tm^{3+} and Ho^{3+} ions was conducted basing on calculated absorption cross-sections of holmium ions and emission cross--sections of thulium ions. The absorption cross-sections were determined from the following dependence:

$$\sigma_{\mathrm{abs}} = \frac{\alpha(\lambda)}{N}, \tag{3}$$

where $\alpha(\lambda)$ — spectral absorption coefficient [cm^{-1}], N — concentration of rare earth elements [ions/cm^3].

As for the emission cross-sections, they were calculated relying on a modified McCumber [12] method which considers mutual relations between absorption and emission cross-sections, as described by the equation

$$\sigma_{\mathrm{em}}(\lambda) = \sigma_{\mathrm{abs}}(\lambda)\frac{g_1}{g_2}\exp\left(\frac{E_0 - \frac{hc}{\lambda}}{kT}\right), \tag{4}$$

where g_1, g_2 denote degree of degeneration of respectively upper and lower multiplet, h is the Planck constant, c — the speed of light, k — the Boltzmann constant, T — ambient temperature, E_0 — energy difference between the lowest levels of split ground-state and excited multiplets [cm^{-1}].

Figure 4 presents the comparison of absorption and emission cross-sections for thulium at the emission wavelength λ_{e} in glass with molar content of Tm_2O_3 equal to 1%. Spectral adjustment of the both cross-sections in

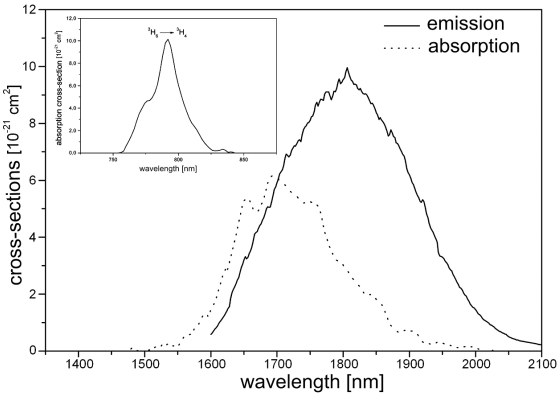

Fig. 4. The absorption and the emission cross-section of Tm^{3+} ion doped antimony silicate glass. (inset) The absorption cross-section of thulium ion at pump wavelength.

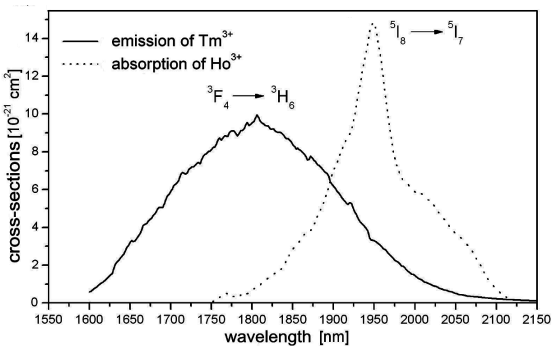

Fig. 5. Emission cross-section of Tm^{3+} ion and absorption cross-section of Ho^{3+} ion doped antimony–silicate glass.

the $^3F_4 \leftrightarrow {}^3H_6$ transition is strongly related to the split ground state leading to the formation of a quasi-four--level system in the structure of Tm^{3+} ions. In this case, higher value of the emission cross-section in comparison to the absorption cross-section allows to obtain considerable amplification in fiber lasers. The inset in Fig. 4 shows characteristics of absorption cross-section for the pump wavelength λ_{p}. The achieved value of absorption cross-section for thulium $\sigma_{\mathrm{e}}(\lambda_{\mathrm{e}}) = 9.51 \times 10^{-21}$ cm^2 is higher than the values typical of silicate glasses [13], and comparable to those of germanium glasses [14].

In the case of glasses doped with both Tm^{3+} and Ho^{3+} ions, probability and efficiency of donor-acceptor energy transfer depends on the spectral adjustment of cross--sections, as well as on the distance between interacting ions. Because of the energy difference between multiplets $^3F_4$ (Tm^{3+}) and $^5I_7$ (Ho^{3+}) amounting to *ca.* 400 cm^{-1}, the produced glasses allowed to obtain quasi-resonant energy transfer $Tm^{3+} \rightarrow Ho^{3+}$. Figure 5 illustrates spectral overlap of the emission cross-section of thulium with the absorption cross-section of holmium in the glass doped with 1 mol.% Tm_2O_3 : 0.75 mol.% Ho_2O_3.

Taking advantage of the relations between absorption and emission cross-sections, the probability of spontaneous emission A_r and radiative lifetime τ_{21} could be determined with (5) and (6):

$$A_r = \frac{8\pi n^2 c}{\bar{\lambda}^4}\frac{g_1}{g_2}\int \sigma_{abs}(\lambda)\,d\lambda, \tag{5}$$

where $\bar{\lambda}$ is a mean wavelength corresponding to the particular radiative transition defined as $\bar{\lambda} = \int \lambda I(\lambda)\,d\lambda \int I(\lambda)\,d\lambda$, with $I(\lambda)$ — spectral distribution of luminescence,

$$\tau_r = \frac{1}{A_r} \tag{6}$$

probability of spontaneous emission A_r as well as radiative lifetime τ_r of the donor excited states (Tm^{3+}) are provided in Table I.

TABLE I

Probability of spontaneous emission and radiative life time of Tm^{3+} ion.

Ion [mol.%]	Manifold	A_r [s^{-1}]	τ_r [ms]
$1Tm_2O_3$	$^3H_4$	12809	0.078
	$^3F_4$	412	2.42

Probability of resonant energy transfer between excited states is described by the Förster–Dexter theory [15–16], in which the dominant role is performed by dipole–dipole type interactions defined accordingly to the mean value of the radius R between doping atoms. In consequence, the following dependence occurs:

$$P_{DA} = \frac{3h^4c^4Q_A}{4\pi R^6 n^4 \tau_D}\int \frac{f_D(E)f_A(E)}{E^4}\,dE, \tag{7}$$

where n — refractive index of the medium, R — mean interionic radius, Q_A — oscillator strength resulting from the total absorption cross-section of the acceptor, τ_D — radiative lifetime of the donor photon, $f_D(E)$ and $f_A(E)$-oscillator strengths related respectively with the donor emission and acceptor's absorption, E — mean photon energy.

With the introduction of the critical radius R_c between the donor and acceptor for which energy transfer efficiency equals 50%, Eq. (7) assumes the form

$$P_{DA} = \frac{1}{\tau_D}\left(\frac{R_c}{R}\right)^6. \tag{8}$$

Efficiency of energy transfer can be then expressed by the equation

$$\eta_{ET} = \frac{P_{DA}\tau_D}{1 + P_{DA}\tau_D}, \tag{9}$$

which, after consideration of the critical radius R_c, can be written as

$$\eta_{ET} = \frac{(R_c)^6}{(R_c)^6 + (R)^6} = \frac{1}{1 + \left(\frac{R}{R_c}\right)^6}. \tag{10}$$

Calculation of either probability or efficiency of energy transfer requires solving the integral of spectral overlap of donor emission and acceptor absorption, as well as establishing oscillator strength resulting from the absorption of acceptor ions. An alternative approach to determining the efficiency of resonant energy transfer involves consideration of changes in donor luminescence intensity ratio in the function of interaction with acceptor absorption field, in which [15]:

$$\eta_{ET} = 1 - \frac{I}{I_0}, \tag{11}$$

where I — luminescence intensity in the donor emission field in the presence of acceptor ions, I_0 — intensity of luminescence lines in the donor emission field with the lack of acceptor ions.

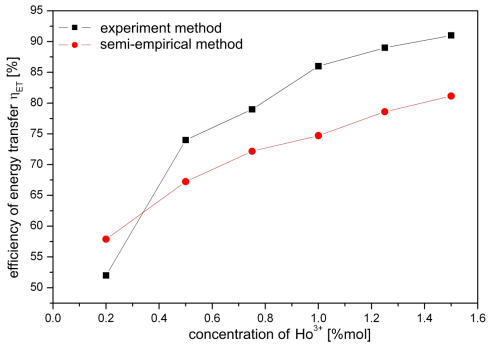

Fig. 6. The efficiency of energy transfer $Tm^{3+} \rightarrow Ho^{3+}$ in antimony–silicate glasses.

Figure 6 illustrates the comparison of energy transfer efficiency in the function of acceptor ion content (Ho^{3+}), calculated relying on the Förster–Dexter theory, as well as obtained in the course of luminescence measurements. Interpreting the character of efficiency changes, it has to be noted that it is similar in both of the cases. In the produced antimony–silicate glass doped with 1 mol.% Tm_2O_3 : 0.75 mol.% Ho_2O_3, marked by the highest level of luminescence at the wavelength within the band of 2 μm, the calculated efficiency equalled 72% and was approximately 10% lower than the efficiency obtained during luminescence measurements. The main reason behind this difference is the character of the interaction which, in the case of the measured value, accounts only for the change in the efficiency of donor quantum emission caused by the Coulomb interaction of the donor-acceptor. By contrast, the efficiency of energy transfer determined by means of the Förster–Dexter theory considers degree of spectral overlap of acceptor absorption cross-section and donor emission cross-section, caused by dipole–dipole interaction and the mean interionic radius R.

3.5. ASE fiber source

Table II contains geometrical parameters of optical fiber made of antimony–silicate glass doped simultaneously with Tm^{3+}/Ho^{3+} ions.

TABLE II

Parameters of manufactured fiber.

Parameter	Value
fiber diameter [μm]	380
active core diameter [μm]	20
numerical aperture NA_r	0.32
off-set [μm]	100

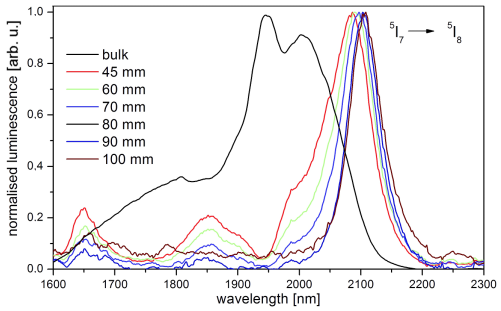

Fig. 7. The emission spectra of 1 mol.% Tm_2O_3 : 0.75 mol.% Ho_2O_3 codoped antimony–silicate fiber and bulk glass excited with 795 nm laser source. The spectra have been normalized with respect to the peak at ≈ 2.0 μm.

By exciting the fiber with radiation at the wavelength of 795 nm, luminescence in the range from 2000 to 2200 nm, resulting from the energy transfer between thulium and holmium ions was achieved.

Figure 7 presents a normalized comparison of spontaneous emission spectra for optical fibers of different lengths with the spectrum of core glass co-doped with the combination of 1 mol.% Tm_2O_3 : 0.75 mol.% Ho_2O_3. Optical trapping of holmium ions related to the distance of the interaction and to the energy confinement in the fiber effected in the narrowing and shifting of the band maximum towards longer wavelengths. Moreover, the phenomenon of radiation reabsorption occurring at the wavelength within the band of 1950 nm, corresponding with the maximum absorption of the $^5I_8 \rightarrow {}^5I_7$ (Ho^{3+}) transition, eliminated the characteristic saddle shape appearing in the luminescence spectrum of the glass doped with Ho^{3+} ions.

The narrowing and redshifting of the emission at the wavelength within the band of 2.1 μm corresponding with the $^5I_7 \rightarrow {}^5I_8$ transition in the energy-level structure of the holmium ion ensued as a consequence of emissions transitions from the same Stark sub-level of the $^5I_7$ multiplet to higher Stark sub-levels of the $^5I_8$ multiplet. Participation of the remaining luminescence bands at the wavelength of 1.46 μm and 1.81 μm originating from the transitions $^3H_4 \rightarrow {}^3F_4$, $^3F_4 \rightarrow {}^3H_6$ in the structure of Tm^{3+} was negligible in the fiber when compared to active glasses. Thus, as a result of effective energy transfer $Tm^{3+} \rightarrow Ho^{3+}$ in the manufactured fiber, narrow and strong bands of amplified spontaneous emission (ASE) were created.

The conducted analysis concerning dislocation of the emission maximum $I_{2\mu m}$ in the band of about 2 μm and of full width at half maximum (FWHM) depending on the fiber length (Fig. 8) proved that in comparison to glass luminescence, in the produced fiber over the length of 100 mm a shift of emission band maximum occurs towards longer wavelengths ($\lambda_e = 108$ nm), accompanied by the narrowing of full width at half maximum ($\Delta\lambda_{FWHM} = 63$ nm).

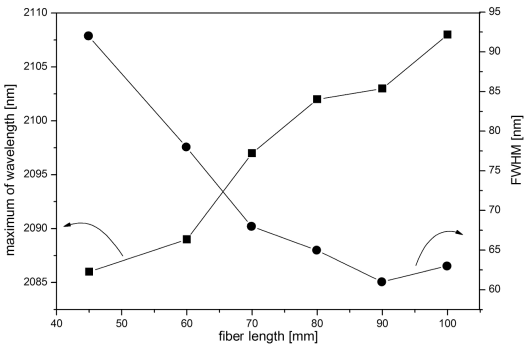

Fig. 8. The maximum emission at 2 μm and $\Delta\lambda_{FWHM}$ as a function of fiber length.

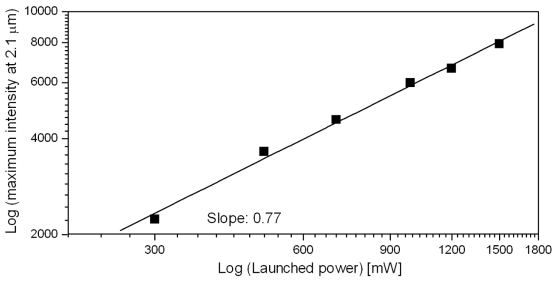

Fig. 9. Measured emission intensity from fiber as a function the launched (and absorbed) power from the laser diode.

Figure 9 presents the intensity of emission within the bandwidth of 2.1 μm in the function of power delivered to the manufactured fiber. The slope of the line indicates that emission efficiency for the $^5I_7 \rightarrow {}^5I_8$ transition in the structure of holmium ions equaled 0.77. As the performed investigation proved, in consequence of effective energy transfer between thulium and holmium ions, in the active core the processes of radiative relaxation corresponding with the $^5I_7 \rightarrow {}^5I_8$ (Ho^{3+}) transition prevailed. The awareness of emission efficiency allows further optimization of the fiber operational conditions, with a view of its possible future applications.

4. Conclusions

Within the scope of the presented research, stable antimony–silicate glasses were obtained and subsequently doped with 1 mol.% Tm_2O_3 and x mol.% Ho_2O_3 (where

x = 0, 0.1, 0.2, 0.5, 0.75, 1.0, 1.25, and 1.5). Analysis of luminescence properties of thus produced glasses proved that optical excitation of the co-doped samples at the wavelength within the band of 795 nm, corresponding with the absorption from the ground state of thulium $^3H_6 \rightarrow {}^3H_4$, enables excitation energy transfer between the donor and acceptor. Because of the energy difference between multiplets $^3F_4$ (Tm^{3+}) and $^5I_7$ (Ho^{3+}) amounting to *ca.* 400 cm^{-1}, the glasses facilitated effective quasi-resonant energy transfer $Tm^{3+} \rightarrow Ho^{3+}$. As a result, strong luminescence was produced with the maximum at the wavelength of 2010 nm, corresponding with the quantum transition $^5I_7 \rightarrow {}^5I_8$ in holmium ions.

By optimizing the doping composition, in the antimony–silicate glass doped simultaneously with 1 mol.% Tm_2O_3 : 0.75 mol.% Ho_2O_3 which was characterized by the highest luminescence level at the wavelength within the band of 2 μm, the efficiency of energy transfer at the level of 80% was achieved. Combining the glass-forming elements with various levels of chemical bonds vibration made it possible to elevate the efficiency of energy transfer between activator ions and, concurrently, allowed to minimize non-linear effects. Furthermore, the presence of a network former guaranteed good thermal stability of the glass, such as required by optical fiber technology.

The optimization of the activator content and of the donor (Tm^{3+})/acceptor (Ho^{3+}) ions concentration ratio which was conducted with the purpose of maximizing the efficiency of energy transfer made it possible to select best-suited glass which was later used to manufacture double-clad fiber. Accordingly, a multimode double-clad fiber whose active core was made of glass with the molar content of $1Tm_2O_3$–$0.75Ho_2O_3$ was produced by means of the standard rod-in-tube method.

By exciting the fiber with radiation at 795 nm wavelength, strong and narrow bands of ASE which formed as a result of energy transfer between thulium and holmium ions were observed. During measurements it was noted that inside the active medium the process of optical trapping in holmium ions took place, causing the shift of the luminescence maximum towards longer wavelengths, as well as the narrowing of the full width at half maximum. In comparison to the luminescence of the glasses, in the produced fiber, over the length of 100 mm, the luminescence maximum was achieved at the wavelength within the band $\lambda_e = 2108$ nm, while the full width at half maximum $\Delta\lambda_{FWHM} = 63$ nm. What is more, the emission efficiency at the wavelength within the band of 2.1 μm in the discussed fiber equalled roughly 0.77. This result denotes significantly greater number of radiative transitions in the $^5I_7 \rightarrow {}^5I_8$ (Ho^{3+}) transition, paving the way for further betterment of optical fiber systems.

Acknowledgments

This work was supported by Ministry of Science and High Education of Poland — grant No. N N507 285636

References

[1] A. Godard, *C.R. Phys.* **8**, 1100 (2007).

[2] B.M. Walsch, *Laser Physics* **19**, 855 (2009).

[3] T. Pustelny, J. Ignac-Nowicka, Z. Opilski, *Opt. Appl.* **34**, 249 (2004).

[4] T. Pustelny, I. Zielonka, C. Tyszkiewicz, P. Karasiński, B. Pustelny, *Opto-Electron. Rev.* **14**, 161 (2006).

[5] R. Balda, J. Fernández, S.G. Revilla, J.M. Navarro, *Opt. Expr.* **15**, 6750 (2007).

[6] M. Reben, J. Wasylak, N.S. alZayes, A.M. El-Naggar, M.G. Brik, I.V. Kityk, *J. Mater. Sci. Mater. Electron.* **23**, 631 (2012).

[7] J.G. Bünzli, Sv.V. Eliseeva, *J. Rare Earths* **28**, 824 (2010).

[8] M. Wanga, L. Yi, G. Wanga, L. Hua, J. Zhanga, *Solid State Commun.* **149**, 1216 (2009).

[9] B. Richards, S. Shen, A. Jha, Y. Tsang, D. Binks, *Opt. Expr.* **15**, 6546 (2007).

[10] S. Tanabe, *C.R. Chim.* **5**, 815 (2002).

[11] K. Barczak, T. Pustelny, D. Dorosz, J. Dorosz, *Europ. Phys. J. Spec. Top.* **154**, 11 (2008).

[12] D.E. McCumber, *Phys. Rev.* **136**, A954 (1964).

[13] B.M. Walsh, N.P. Barnes, *Appl. Phys. B* **78**, 325 (2004).

[14] R.R. Xu, Y. Tian, M. Wang, L.L. Hu, J.J. Zhang, *Appl. Phys. B* **102**, 109 (2010).

[15] T. Förster, *Ann. Phys.* **6**, 55 (1948).

[16] D.L. Dexter, *J. Chem. Phys.* **21**, 273 (1953).